HHS Public Access

Author manuscript

J Immunol. Author manuscript; available in PMC 2019 December 10.

Published in final edited form as:

J Immunol. 2018 July 01; 201(1): 230–242. doi:10.4049/jimmunol.1701216.

Innate recognition of the microbiota by Toll-like Receptor-1 promotes epithelial homeostasis and prevents chronic inflammation

Karishma Kamdar[*], **Andrew M. F. Johnson**[+], **Denise Chac**[+], **Kalisa Myers**[*], **Vrishika Kulur**[*], **Kyle Truevillian**[+], **R. William DePaolo**[+,*]

[*]Department of Microbiology and Immunology, Keck School of Medicine, University of Southern California, Los Angeles, CA 90033

[+]Division of Gastroenterology Department of Medicine, University of Washington, Seattle, WA 98105

Abstract

There is crosstalk between the intestinal epithelium and the microbiota that functions to maintain a tightly regulated microenvironment and prevent chronic inflammation. This communication is partly mediated through the recognition of bacterial proteins by host encoded innate receptors, such as Toll-like Receptors. However, studies examining the role of Toll-like Receptor signaling on colonic homeostasis have given variable and conflicting results. Despite its critical role in mediating immunity during enteric infection of the small intestine, TLR1-mediated recognition of microbiota-derived ligands and their influence on colonic homeostasis has not been well studied. Here, we demonstrate that defective TLR1 recognition of the microbiome by epithelial cells results in disruption of crypt homeostasis specifically within the secretory cell compartment, including a defect in the mucus layer, ectopic Paneth cells in the colon and an increase in the number of rapidly dividing cells at the base of the crypt. As a consequence of the perturbed epithelial barrier, we found an increase in mucosal-associated and translocated commensal bacteria and chronic low-grade inflammation characterized by an increase in lineage-negative, $Sca1^{+}Thy1^{hi}$ innate lymphoid-like cells that exacerbate inflammation and worsen outcomes in a model of colonic injury and repair. Our findings demonstrate that sensing of the microbiota by Toll-like Receptor-1 may provide key signals that regulate the colonic epithelium thereby limiting inflammation through the prevention of bacterial attachment to the mucosa and exposure to the underlying immune system.

Correspondence: R. William DePaolo, Associate Professor of Medicine, Department of Medicine, University of Washington, Seattle, WA 98195, Phone: 206-616-7227, wdepaolo@medicine.washington.edu.

AUTHOR CONTRIBUTIONS

VK performed experiments, KM performed all the immunohistochemistry, KK performed experiments, analyzed and interpreted data, AMFJ performed experiments, analyzed and interpreted data, and revised the manuscript, DC performed bioinformatics analysis of 16s rDNA sequencing, KT quantified histology, RWD conceived the study, analyzed and interpreted data and wrote the manuscript.

COMPETING FINNCIALINTERESTS

The authors declare no competing financial interests.

Keywords

Mucosal immunology; TLR; gut microbiome

INTRODUCTION

The intestinal epithelium is the major interface between the 100 trillion commensal bacteria that comprise our gut microbiome and the immune cells found within the lamina propria (LP). The interactions between the gut microbiota and the epithelium shape important biological processes such as metabolism, development of the mucosal-associated tissues and immunity against invading pathogens (1–4). Despite the extraordinary microbial burden within the intestine, translocation across the epithelium is a rare event due to the highly specialized cells that form this barrier. Tightly regulated communication via the direct sensing of the microbiome by innate immune receptors encoded within the epithelium is important for the homeostasis of the intestine. This process is mediated by the recognition of commensal ligands by host receptors, such as the Toll-like receptors (TLRs) (5–7) and the Nod-like receptors (NLR) (8–10) and the presence of gut bacteria has been shown to impact the rate of proliferation within the stem cell compartment of the intestinal crypt (5, 8, 11–16). Genetic and environmental factors, such as infection, can also influence the dialogue between the microbiota and epithelium, leading to alterations in proliferation, generation of inflammation and bacterial translocation (15, 17, 18) traits shared with the two types of inflammatory bowel disease (IBD), Crohn's disease and ulcerative colitis (16, 19, 20).

TLRs and NLRs are expressed throughout the intestine and have been identified on crypt and intestinal stem cells (ISC) (17, 19, 21–24). TLR signaling mediates a number of cellular responses (1, 22) and can be classified into two groups based upon the intracellular signaling adaptor. TLR1, −2, −5, −6 and −10 signal through the myeloid differentiation primary response gene-88 (MyD88), while TLR3, −4 and −9 signal through the TIR-domain-containing adapter-inducing interferon-β (TRIF)-dependent pathways (1, 19, 22–24). Studies disrupting innate signaling in mice, either through deletion of a specific TLR or through MyD88, have shown that sensing of the microbiota via these receptors is critical in mediating their own epithelial expression, regulating epithelial proliferation, and in the response to intestinal injury (23, 25, 26). TLR2, which is expressed throughout the small intestine and colon (14, 25, 27), recognizes lipoproteins from gram-positive and gram-negative bacteria, as well as zymosans from yeast. TLR2 achieves this heterogeneity in ligand recognition by dimerizing with other TLRs, such as TLR1, −6 and −10. Major functions attributed to TLR2 in the maintenance of intestinal epithelial integrity is through the regulation of tight junctional proteins, proliferation/apoptosis signals (23, 26), antimicrobial peptide expression (25, 27), and goblet cell activation (28–30). While these studies have shed light on the role of TLR2, they have not delineated whether TLR2 signaling alone is sufficient to drive these processes, or if other binding partners may be contributing to its effect. Recently, our group has shown that TLR1 is important in coordinating cellular immunity against infection of the small intestine by *Yersinia enterocolitica* (15, 17, 18). Despite elimination of *Y. enterocolitica*, TLR1-deficiency promotes dysbiosis of the microbiota and the development of chronic anti-commensal

immune sequela (18). Therefore, disrupted innate immunity against an enteric pathogen may have long-term consequences and may promote the development of chronic inflammatory disease.

Here, we show that disruption of TLR1 signaling compromises the colonic epithelium, leading to innate immune activation and chronic inflammation. Upon colonic injury the chronic inflammatory state prevents healing and promotes more severe disease suggesting that endogenous sensing of the microbiota through TLR1 contributes to colon homeostasis and prevents epithelial and immune dysfunction.

MATERIALS & METHODS

Mice

TLR1KO (1KO), TLR1 Heterozygote, and TLR1 wildtype mice (WT) mice were generated through the breeding of 1KO males with wildtype or heterozygous females. Litters were mixed upon separation and genotypes were cohoused together in cages through the duration of all experiments unless stated otherwise in the figure legend or methods. Mice were maintained at the University of Southern California and the University of Washington, and experiments were performed following protocol review and approval by the Institutional Biosafety Committee and the Institutional Animal Care and Use Committee. Mice were housed in specific-pathogen-free conditions, administered sterile, non-chlorinated, non-acidified water and fed a normal mouse chow (AIN-76) *ad libitum*. The mice in this colony are *Helicobacter hepaticus*-free and clear of other pathogens, such as murine Norovirus or *Pasteurella*. Rag2KO mice (B6(Cg)-*Rag2*$^{tm1.1Cgn}$/J) were purchased from Jackson Laboratory (Bar Harbor, ME) and mated with 1KO mice for at least 10 generations prior to use.

DSS treatment

5- to 7-week-old female mice received 2.5% (w/v) dextran sulfate sodium (DSS; Affymetrix, Santa Clara, CA, molecular weight 35,000–50,000 kDa) in drinking water for 7 days followed by 7 days of regular drinking water.

Immuno-histochemistry and Immune-fluorescence

Murine colons were rolled using the Swiss roll technique and fixed in 10% neutral buffer formalin (VWR International, Visalia, CA) or methacarn fixative (VWR) overnight. For preservation of the mucus layer colon pieces with contents were placed in methacarn fixative (60% dry methanol, 30% chloroform, 10% glacial acetic acid) overnight. Methacarn pieces were washed twice in 100% methanol, once in 100% ethanol, and twice in xylene prior to paraffin embedding. Paraffin-embedded (without formalin) tissues were cut 5 μm thick. Hematoxylin and eosin, Alcian blue, mucicarmine and Periodic Acid Schiff staining was performed by AML labs (Saint Augustine, FL) or in-house using Alcian blue pH 2.5 according to manufacturer's instructions (Abcam, Cambridge, MA). Quantification of mucus layer thickness and mucin vesicles were conducted by an individual blinded to the experiment groups. Muc2 (1:200, Abcam, ab76774), BrdU, Ki67 (1:500, NOVUS, MKI67), Gob5 (1:50, Santa Cruz, M-53), lysozyme (1:200, Abcam, Cat# ab108508), alpha defensin-1

(1:2000, kind gift from A. Ouellette), Rabbit polyclonal IgG, (1:200, Abcam, ab27472), rabbit monoclonal IgG (1:200, Abcam, ab172730).

For antigen retrieval, slides were placed into tubes containing sodium citrate buffer (pH 6.0) (Sigma-Aldrich, St. Louis, MO) buffer and heated at 99°C in water bath. The slides were washed and blocked before staining with primary antibody. The slides with primary antibody were incubated overnight at 4°C in a humid chamber and the following day, washed and incubated with secondary at 37°C for 1 hour. The slides were mounted with DAPI and confocal images were acquired using a Nikon Eclipse C1 laser-scanning microscope (Nikon, PA) fitted with a 60 Nikon objective (PL APO, 1.4NA) and Nikon image software.

H&E stained colonic tissue sections were scored by a blinded gastroenterologist using the following measures: crypt architecture (normal, 0 - severe crypt distortion with loss of entire crypts, 3), degree of inflammatory cell infiltration (normal, 0 - dense inflammatory infiltrate, 3), muscle thickening (base of crypt sits on the muscularis mucosae, 0 - marked muscle thickening present, 3), goblet cell depletion (absent, 0- present, 1) and crypt abscess (absent, 0- present, 1). The histological damage score is the sum of each individual score.

Colonic epithelial cell and lamina propria isolation

The colon was removed, flushed with ice cold PBS and 1 mM DTT (Sigma-Aldrich) and shaken at 37°C in HBSS containing 2 mM EDTA (Sigma-Aldrich,) and 2 mM DTT (Sigma-Aldrich) for 10 minutes and the supernatants were collected. This was repeated and supernatants were pooled together and constitute the epithelial fraction. The remaining tissue was digested with collagenase type IV (Sigma-Aldrich) in RPMI with 20% FBS (GE Healthcare, Logan, UT) for 20 minutes. The supernatants were collected, passed through 70 μM mesh filters (BD Biosciences, San Jose, CA) and washed in ice cold PBS.

Detection of bacterial 16S rDNA using RT-PCR and by plating

16S rDNA was analyzed as previously described (9, 31) (9, 31). Briefly, the DNA from colonic mucosa, stool or colonic lumen was extracted using the QIAamp DNA stool kit (Qiagen, Germantown, MD) and two microliters of bacterial DNA was used as a template. The gene copy number per microliter of DNA was determined using plasmids expressing the target of the 16S primers (31). For enumeration of bacteria using standard plating techniques, spleen and liver were aseptically removed and homogenized in 1 mL sterile pre-reduced oxygen free tryptic soy agar (Anaerobe, Morgan Hill, CA). Samples were serially diluted and plated in duplicate and placed in anaerobic jars (Sigma-Aldrich). Forty-eight hours later the colonies were enumerated and compared to plates grown in the presence of oxygen.

Bone marrow chimeras

Mice were irradiated with 1,000 cGy. The mice were immediately reconstituted intravenously with 10×10^6 cells isolated from indicated donor bone marrow. The mice recovered for 6 weeks prior to use.

Fecal Microbiota Transplants

Mice were treated with a cocktail of five antibiotics neomycin (1 g/L, Sigma), amoxicillin (1 g/L, VWR), gentamicin (1 g/L), vancomycin (0.5 g/L, VWR), metronidazole (1 g/L, VWR) in their drinking water for two weeks and received 150 μL of stool contents from indicated donor by oral gavage every other day for a total of 3 total gavages. The mice were left undisturbed for up to 4 weeks before any procedures were performed.

Anti-Thy1, anti-IL-22, anti-IL-17 and anti-IFN-γ treatment

TLR1-sufficient and -deficient Rag2KO mice were administered 1 mg of anti-Thy1 depleting mAb (YTS 154.7.7.10) or rat isotype control (YKIX 337.217.1); 500 μg anti-IL-17A (rat IgG2a; MAB421 R&D; clone 50104), 500 μg anti-IL-22 (rat IgG2a; 16-7222-85 eBioscience; clone IL22JOP); 500 μg anti-IFN-γ (rat IgG1; 505802 Biolegend; clone XMG1.2) intraperitoneally the day of DSS administration and then every other day through day 8.

Intestinal permeability and endotoxin measurement

FITC-conjugated dextran (4,000 MW) dissolved in water (Sigma-Aldrich) was administered rectally to anesthetized mice at 2 mg per 10 grams of body weight using a Foley catheter. Whole blood was collected using heparinized needles via cardiac puncture 1 hour after FITC-dextran administration. Fluorescence intensity in sera was analyzed using a standard plate reader and determined by comparison to a FITC-dextran standard curve. Bacterial endotoxin in the serum was assayed using an endpoint chromogenic LAL assay (Lonza, Anaheim, CA) per manufacturer's instructions.

Quantitative real-time RT-PCR

RNA was extracted from mucosal scrapings, isolated lamina propria, intestinal epithelial cells or sorted $lin^{-}Sca1^{+}Thy^{hi}$ cells using ISOLATE II RNA Mini Kit (Bioline, Boston, MA). RNA was reverse-transcribed into cDNA with SensiFAST™ cDNA Synthesis Kit (Bioline). qPCR was performed on a CFX96 Touch™ Real-Time PCR Detection System (Bio-Rad Laboratories, Irvine, CA) using SensiFAST™ SYBR® No-ROX Kit (Bioline). No reverse transcriptase and water controls are performed for each sample. Data is normalized to product amplified using primers for a housekeeping gene, GAPDH.

Antibodies, flow cytometry and cell sorting

The following conjugated antibodies were used: Sca1 (D7), Thy1 (G7), γδ TCR (GL3), our lineage negative panel contained: CD11c (HL3), Gr-1 (Rb8-6CF), CD11b (M1/70), NK1.1 (PK136), CD19 (1D3), CD8a (53-6.7), CD3e (2C11), CD4 (RM4–5), B220 (RA3-6B2) from BD Pharmingen (San Jose, CA). Flow cytometry analysis was performed with a FACS Canto (BD Biosciences) and analyzed using FlowJo software (FlowJo LLC, Ashland, OR). For sorting, the lamina propria for 5–8 mice were pooled and stained with APC-conjugated lineage markers, followed by labeling with anti-APC beads (Miltenyi, San Diego, CA) and negative sorting on AutoMacs (Miltenyi). Enriched cells were stained with SCa1 and Thy1.2 and sorted on a FACSAria (BD Biosciences).

Detection of cytokines by ELISA

After isolation of the lamina propria, the pellet was homogenized in 2 mL of PBS and protein was quantified using Quick Start™ Bradford Protein Assay (Bio-Rad Laboratories,). Cytokine levels in 50 μg/mL of protein was determined using ELISA assays for IL-1β (BD), IL-23 (BD), IL-12p70 (BD), IL-17 (R&D, Minneapolis, MN), and IL-22 (eBioscience, San Diego, CA).

Measurement of Reactive Oxygen Species (ROS

Fresh mucosal scrapings were collected into pre-weighed tubes and homogenized at 40mg/ml in sterile PBS. ROS was measured in supernatant using the OxiSelect ROS/RNS assay kit (Cell Biolabs, San Diego, CA) according to manufacturer's instructions.

Microbiota composition analysis by 16s rDNA sequencing

Cecal contents from littermate 1KO and WT mice were snap frozen on collection. Genomic DNA was extracted from samples using the Qiagen MagAttract Powersoil DNA Isolation Kit Optimized for the KingFisher (Qiagen Inc., Valencia, California) following manufacturer's protocol at RTLGenomics (Lubbock, TX). Samples were amplified for sequencing at RTLGenomics (Lubbock, TX) in a two-step process, using primers 515F GTGCCAGCMGCCGCGGTAA and 806R GGACTACHVGGGTWTCTAAT (32) and sequenced using the MiSeq platform (Illumina, San Diego, CA). Sequencing data were curated using mothur using the MiSeq standard operating procedure (33). Sequences were then classified using the Ribosomal Database Project v 14 and phylotyped to the genus level. Sequence data was deposited in the Sequence Read Archive (SRA) under accession number SRP143628 (https://www.ncbi.nlm.nih.gov/sra/SRP143628).

Statistics

All data are expressed as mean ± SEM. Differences were considered significant at $p < 0.05$, using a Student's t test (2-tailed), ANOVA test or Wilcoxon Log Rank test as appropriate, and performed with the statistical analysis software Prism (GraphPad Software). Statistical tests and p values are specified in the Fig. legends.

Study Approval

All mice were maintained at University of Southern California or University of Washington Seattle, and experiments were performed following protocol review and approval by the Institutional Biosafety Committee and the Institutional Animal Care and Use Committee.

RESULTS

TLR1-deficiency is associated with mucosal-associated bacteria, gut permeability and systemic bacteria

Our previous work had shown a critical role for TLR1 signaling in the epithelium of the small intestine during pathogenic *Yersinia* infection (18, 22, 34). However, analysis of mRNA transcripts for *Tlr1* in naïve WT mice revealed that the ileum had significantly less expression of *Tlr1* than the proximal colon or distal colon (data not shown). We sought to

determine whether the expression of TLR1 may influence colonic homeostasis by assessing the location of the microbiota within the colonic compartment of TLR1-deficient (1KO) and littermate control mice (a mixture of heterozygotes and homozygotes for TLR1, WT) using fluorescent *in situ* hybridization (FISH) to visualize bacteria with a probe directed against eubacterial 16S rRNA. While we observed a clear separation between cells of the epithelium and the 16S rRNA probe in WT colons, this spatial separation was not observed in the 1KO mice (Fig. 1A). Instead, we observed a diverse spectrum of 16S rRNA expression, including areas where the probe was in intimate contact with epithelial cells (Fig. 1A). The increase in epithelial adjacent bacteria in the 1KO mice corresponded with 15-fold more 16S DNA associated with the mucosa than in the WT mice, despite equivalent luminal levels (Fig. 1B). To assess whether there was also altered colonic permeability, fluorescein isothiocynate (FITC)-labeled dextran was measured in the peripheral blood of WT and 1KO mice one hour after intra-rectal administration. Indeed, there was a significant increase in the amount of FITC in the blood of the 1KO mice, indicating leakage from the colon into the periphery (Fig. 1C), as well as elevated endotoxin levels suggesting translocated commensal bacteria or their products (Fig. 1D). To determine the extent of bacterial translocation in 1KO mice, spleen, liver and blood were plated anaerobically on tryptic soy agar (TSA) plates. The liver (Fig. 1E–F), spleen and blood (data not shown) from 1KO mice all had significantly elevated amounts of bacteria compared to littermates. Further, the transfer of TLR1-deficient bone marrow to reconstitute an irradiated WT mouse was not sufficient to cause an increase in bacterial colonies in liver (data not shown), indicating that the elevated levels of systemic bacteria in the naïve 1KO mice are not due to an ineffectual immune response against mouse pathogens that may be resident in SPF facilities. Gut permeability may result from defects in the regulation of tight junctional proteins and previous studies have implicated TLR2 in this regulation (10, 21). However, using quantitative PCR we were unable to find any difference in the expression of *Cldn3* (claudin-3), *Cldn10* (claudin-10), *Ocln* (occludin) and *Tjp1* (ZO-1) transcripts (data not shown). We also quantified claudin-2 and claudin-3 by Western blot and assessed occludin-1 expression by immune-fluorescence and observed no differences between 1KO and WT mice (Supplemental Fig. 1). Altogether, these data demonstrate an inability to maintain normal geographical and spatial localization of commensal bacteria in the absence of TLR1 independent of barrier defects.

Elevated innate immune responses in TLR1-deficient mice

Mucosal-associated and translocated commensals are often associated with inflammation due to increased exposure to, and subsequent recognition by, the immune system. As the 1KO mice have inherent bacterial translocation, we evaluated cytokine levels in homogenates of whole colon by ELISA (Fig. 2A). Of the ten cytokines we evaluated, only IL-1β and IL-23 and the cytokines they play a role in regulating, IL-22 and IL-17 (27, 35, 36), were significantly increased in the colons of the 1KO (Fig. 2A).

There are three IL-23-responsive cells that produce IL-22 and IL-17 within the colonic mucosa. These include γδ T cells (36–38), IL-17-producing CD4 T cells (T_H17/T_H22) (19) and type 3 innate lymphoid cells (ILC3) (39). We sought to identify the frequency of these cell populations in naïve mice and found no difference in the frequency or numbers of γδ T cells (Fig. 2B) and T_H17 cells (Fig. 2C) between 1KO and WT controls (Fig. 2B). However,

the frequency (Fig. 2D) and absolute cell number (Fig. 2E) of lineage negative (lin^-) $Sca1^+Thy1^{hi}$ cells in the colons of the 1KO mice were significantly elevated compared to naïve WT controls (Fig. 2D–E). Lineage negative, Sca1 and Thy1-positive cells have been identified as IL-22 and IL-17-producing ILC3 (16). Molecular analysis of the mRNA transcripts from sorted $lin^-Sca1^+Thy1^{hi}$ cells revealed prototypic molecular signatures of ILC3, such as *Rorc* (Fig. 2F), *Il22* (Fig. 2G) *Il17*, and *Il23r* (data not shown), to be increased in 1KO compared to WT cells, while *Ifng* expression was not changed (Fig. 2G).

TLR1-sensing of the microbiota by non-hematopoietic cells restrains innate immune responses

Despite the proximity of commensal bacteria to colonic tissue in healthy individuals, there are conflicting reports regarding the role of the microbiota in the development of members of the ILC family. To determine whether the microbiota was necessary for innate immune activation in the 1KO mice, we employed a rigorous antibiotic treatment regimen to deplete the microbiota. Pregnant dams from a heterozygous cross were administered a cocktail of 5-antibiotics (amoxicillin, vancomycin, neomycin, metronidazole, and gentamicin) (ABX) the last week of their pregnancy and maintained on the ABX–water until the pups were weaned. The newly weaned mice continued to receive the ABX-water for an additional seven days, at which time their colons were analyzed for levels of IL-23 and $Sca1^+Thy1^{hi}$ cells. This antibiotic approach generally yields a 5–8 fold reduction in the endogenous commensals (unpublished observations). While ABX treatment had little effect on the basal level of $Sca1^+Thy1^{hi}$ cells in WT mice, it significantly reduced the number of these cells (Fig. 3A) along with colonic level of IL-1β and IL-23 (Fig. 3B) in the 1KO mice. As the microbiota was necessary for the elevated innate immune response, we asked whether the specific composition of the microbiota of 1KO mice would be sufficient to transfer this phenotype to ABX-treated WT mice via fecal microbiota transplantation (FMT). WT mice receiving an FMT with stool from a 1KO mouse showed no change in either the $lin^-Sca^+Thy1^{hi}$ population (Fig. 3C) or levels of IL-1β and IL-23 (Fig. 3D). In contrast, WT stool given to an ABX-treated 1KO recipient restored both the $lin^-Sca1^+Thy1^{hi}$ population (Fig. 3C) and IL-1β and IL-23 (Fig. 3D).

These data suggest that while bacteria are necessary for the colonic inflammation observed in the 1KO mice, the lack of signaling through TLR1 does not alter the microbiota to cause inflammation when transferred to a WT setting. This was further supported by comparing the 16s rDNA sequencing analysis of cecal contents between 1KO and WT mice. Principal coordinate analysis (PCoA) (Fig. 3E) and inverse-Simpson index (Fig. 3F) indicated considerable overlap in community structure and no difference in community α-diversity between naïve WT and 1KO mice, respectively. Differences in the relative abundances of bacterial families in the cecum of 1KO and WT mice were evaluated by Student's *t* tests corrected for multiple testing using the Benjamini and Hochberg false discovery rate (set at 5%). Consistent with the α-diversity and PCoA, there were no significant differences in bacterial families between 1KO and WT mice (Fig. 3G). To confirm the results obtained using cecal contents and to evaluate specific biogeographical changes in the bacterial community of the colon, we performed compositional analysis on mucosal-associated tissue from the proximal and distal colon in a subset of 1KO and of WT mice. PCoA of the 16S

rDNA data again revealed no significant differences in these mucosal-associated communities between 1KO and WT mice (Supplemental Fig. 2). Thus, it is unlikely that the aberrant immune response observed in the 1KO mice is due to a compositional shift in the microbial communities within the colon.

The finding that 1KO mice had elevated innate cytokines and increased $lin^{-}Sca1^{+}Thy1^{hi}$ cells after receiving WT stool and the lack of a compositional change in the microbiota of 1KO mice suggests that the dysregulation of the innate immune response may be due to a more general defect in the mucosal response to commensal bacteria. Previously, we have shown that TLR1 can signal in both the intestinal epithelium and in mucosal dendritic cells (DC) to induce protective immunity against enteric infections (22, 34). To discern which cellular compartment may be mediating the elevated innate immune activation we created bone marrow chimeras. Two months after reconstitution, IL-1β and IL-23 concentration in the colonic LP and the bacterial burden in the liver were quantified. The transfer of 1KO bone marrow to WT mice had no effect on colonic LP levels of IL-1β or IL-23 (Fig. 4A) and no increase in bacterial burden was observed (Fig. 4B). In contrast, IL-1β and IL-23 (Fig. 4A) were elevated in the LP and there was an increase in bacterial counts (Fig. 4B) when 1KO recipients were reconstituted with WT bone marrow. These data suggest that non-hematopoietic cellular expression of TLR1 prevents commensal-mediated inflammation and bacterial translocation. Together, the FMT and bone marrow chimera studies establish that defective TLR1-sensing of the microbiome by non-hematopoietic cells, and not a compositional dysbiosis, is responsible for the innate inflammatory phenotype observed the 1KO mice.

TLR1 signaling contributes to homeostasis of the colonic epithelium

The intestinal epithelium is comprised of a single layer of cells that form a physical barrier between us and our microbiota. The epithelium is comprised of specialized intestinal epithelial cells (IEC). The four types of IEC are derived from a single crypt progenitor but have distinct developmental pathways. Using immunohistochemistry and gene expression, we evaluated key markers and products of differentiated IEC. Goblet cells are one of the four types of IEC and function to produce a physical mucus barrier. WT colonic sections stained for Muc2, the main peptide component of intestinal mucins, revealed a visible mucus layer and characteristic goblet cell staining (Fig. 5A). In contrast, 1KO mice had large areas completely devoid of MUC2 and there was a lack of intensity in the positively stained goblet cells (Fig. 5A). Further analysis using Alcian blue (AB) and mucicarmine staining revealed a reduction in acidic mucins in the colons of 1KO mice, while Periodic Acid Shift (PAS) staining of neutral mucins appeared more similar between 1KO and WT (Fig. 5A). The reduction in acidic mucins was not due to an exocytosis of the whole endocytic granule, as we were unable to find PAS, PAS/AB or AB positive cells in the lumen, a phenotype recently observed in $NLRP6^{-/-}$ mice (40). However, using confocal microscopy, we did observe a strong reduction in the expression of GOB5, which is found on the outer surface of mucus containing granules, (Fig. 5A). The thickness of the mucus layer was measured at multiple points around distal colonic sections stained with Alcian blue to quantify any differences between 1KO and WT mice (Fig. 5B). Quantification revealed a significant reduction in the average thickness of the mucus layer in 1KO compared to WT mice (Fig.

5C). Changes in the mucus layer may be due to either a defect in the production or the secretion of mucus by cells within the crypt. Quantification of the number of Alcian blue positive vesicles per crypt indicated an accumulation of mucus within the epithelial cells of 1KO mice (Fig. 5D). Recently it has been shown that mucus secretion by sentinel goblet cells in the colon can be induced by TLR1/2 agonism via a mechanism dependent on reactive oxygen species (ROS) (29). Consistent with this pathway, we found significantly reduced levels of ROS in the colonic mucosa of the 1KO mice relative to WT counterparts (Fig. 5E).

Under chronic stress or inflammatory conditions the colon, which is normally devoid of Paneth cells, will express Paneth cell products and these cells are referred to as ectopic Paneth cells (41–43). To determine whether the chronic inflammation observed in the 1KO mice was causing a re-programming of the colonic crypt, we compared the expression of two products normally secreted by small intestinal Paneth cells, lysozyme (Lyz) and α-defensin-1 (DEFA-1). As expected, lysozyme expression in the colon of healthy, naïve WT mice was very low (Fig. 5F), while exposure matched images of colons from 1KO mice demonstrated high expression of lysozyme at the top of the crypts (Fig. 5F). WT mice expressed a gradient of DEFA-1 which increased basolaterally (Fig. 5F) and was absent in the 1KO mice (Fig. 5F). instead the whole crypt stained uniformly positive for DEFA-1 (Fig. 5F). Taken all together, the absence of TLR1 signaling is associated with alterations in the production and function of factors associated with secretory cells of the epithelium.

TLR1 signaling restrains microbiota-induced epithelial cell proliferation

IEC differentiation is a tightly regulated process involving many important factors that control cellular proliferation, as well as differentiation. We began by examining the proliferation of the epithelial cells in naïve WT and 1KO mice. Ki67 is a marker used to identify cells that are currently, or have recently, undergone proliferation by labeling cells in S, G_1, and G_2 phases of the cell cycle. Histological analysis of colonic tissue sections of naïve mice revealed an increase in Ki67-positive cells within the colonic epithelium of 1KO mice when compared to WT mice (Fig. 6A). In the colon, rapidly cycling stem cells at the base of the colonic crypt control proliferation and renewal of the epithelium. Aberrant regulation of these crypts may lead to altered IEC differentiation and disrupt epithelial barrier integrity. We used *in vivo* injections of bromodeoxyuridine (5-bromo-2'-deoxyuridine, BrdU) to label newly synthesized DNA in actively replicating cells during S phase for two and a half hours. Analysis of BrdU-positive cells by immunohistochemistry confirmed the presence of three to four BrdU-positive cells per WT crypt, (Fig. 6B–C). In contrast, mice deficient for TLR1 had twice the number of BrdU-positive cells per crypt (Fig. 6B–C). Cyclin D1 is a factor downstream in the Wnt signaling cascade, involved in cell cycle regulation (5). As expected based upon the Ki67 and BrDU data, transcripts for *Ccnd1* (cyclin D1) were elevated in the colonic tissue of 1KO mice (Fig. 6D).

Antibiotic-depletion was used to assess whether the proliferation in the colonic crypt of the 1KO mice was dependent upon the microbiota. Reducing the bacterial load caused a significant reduction in overall Ki67 (Fig. 6A), BrdU staining (Fig. 6B–C), and *Ccnd1* expression (Fig. 6D) in the colons of the 1KO mice. These data suggest that TLR1

expression may antagonize or inhibit other innate signals that promote proliferation, or TLR1 regulates the stem cell niche. To test for the latter, we analyzed expression of canonical stem cell genes (*Lgr5, Bmi1*) and Notch signaling genes that regulate cell differentiation along absorptive and secretory pathways (*Notch1, Hes1, Atoh1*) and found no differences between 1KO and WT mice (Supplemental Fig. 3).

TLR1 deficiency exacerbates tissue injury and prevents epithelial healing

Basal changes in mucosal and epithelial homeostasis may set the stage for sustained inflammation and chronic intestinal disease following intestinal injury. We sought to determine whether the absence of TLR1 during injury caused by 2.5% dextran sodium sulfate (DSS) may induce a more chronic, long-term inflammatory response. 1KO and WT mice were given 2.5% DSS in their drinking water for seven days followed by a seven-day recovery period where normal drinking water was restored. The WT littermate controls followed the typical disease course known for DSS with a transient, mild weight loss (Fig. 7A), very high survival (Fig. 7B) and a shortening of the colon observed at day 7 which returns to normal length by day 14 (Fig. 7C). In contrast, 1KO mice began losing weight earlier than WT controls, lost more weight (Fig. 7A) and had only 30% of mice survive treatment (Fig. 7B). The 1KO mice also had shorter colons at both days 7 and 14 (Fig. 7C) and had higher levels of blood in their stool, which persisted throughout the 14 days (Fig. 7D).

Histological scoring was performed blinded by gastroenterologist on hematoxylin and eosin stained colonic tissue after injury (day 7) and after repair (day 14). Despite a greater weight loss and less overall survival, the histological score was strikingly similar between the 1KO and WT mice at day 7 (Fig. 7E & data not shown). At day 14, after the mice had been returned to normal drinking water, the histological score of WT mice was improved compared to day 7, indicating effective mucosal repair and resolution (Fig. 7F). In contrast, the colons of 1KO mice showed little resolution at day 14 and, in fact, scored significantly worse than at day 7 (Fig. 7E) with large areas of denuded epithelium, inflammatory cell infiltrate and loss of goblet cells (Fig. 7F).

Whole colonic tissue was collected at days 0 and 10 for analysis of IL-1β, IL-23 and IL-12. Consistent with our earlier data, colonic tissue from naïve 1KO mice had higher levels of IL-1β and IL-23, but not IL-12p70 (Fig. 7G). After receiving DSS for 7 days and normal drinking water for three days there was an increase in the amount of IL-1β and IL-23 in both WT and 1KO mice, with significantly higher levels found in the 1KO (Fig. 7G). Interestingly, IL-12p70 was only detected at day 10 in the colonic homogenate of 1KO mice (Fig. 7G). To assess the IL-23-dependent production of IL-22 and IL-17, colonic explants were performed on tissues harvested at the same time points and re-stimulated *in vitro* with recombinant IL-23. Colons from naïve WT mice produced detectable IL-22 only in the presence of rIL-23 but failed to produce IL-17 (Fig. 7H). In contrast, the unstimulated colon explants from naïve 1KO produced detectable IL-22 and IL-17 that was further increased by the addition of rIL-23 (Fig. 7H). Seven days after initial DSS exposure and three days into the repair cycle, IL-22 and IL-17 were elevated in the 1KO explants stimulated with the vehicle control and the addition of rIL-23 significantly increased these levels (Fig. 7H).

Interestingly, IFN-γ levels were not detected in the colons from naïve WT and 1KO mice, yet after DSS exposure IFN-γ production was significantly increased in the cultures containing colons from the 1KO mice (Fig. 7G). Analysis of the major colonic IL-23R responsive cells in the mice at day 7 of DSS revealed elevated numbers of $Sca1^{+}Thy1^{hi}$ cells in both WT and 1KO mice, yet were significantly higher in the 1KO mice, while the numbers of γδ T cells and T_H17 cells did not increase (Fig. 7I).

To determine if the severe pathology and inability to recover from intestinal injury in the 1KO mice was due to elevated numbers of $Sca1^{+}Thy1^{hi}$ cells these mice were bred onto a RAG2-deficient (RagKO) background, allowing us to deplete $Sca1^{+}Thy1^{hi}$ cells using a polyclonal antibody against Thy1. Confirming our results in Fig. 7, the absence of TLR1 in RagKO mice resulted in a much more rapid and severe weight loss (Fig. 8A), significantly less survival (Fig. 8B), and a shorter colon length (Fig. 8C) than TLR1-sufficient RagKO mice. Administration of the anti-Thy1 antibody significantly improved the disease outcome in the DSS-treated RagKO mice with less weight loss (Fig. 8A), less mortality (Fig. 8B) and longer colon lengths (Fig. 8C). TLR1-deficient RagKO mice treated with anti-Thy1 also had significantly less IL-22 (Fig. 8D), IL-17 (Fig. 8E) and IFN-γ (Fig. 8F) than control antibody-treated TLR1-deficient RagKO mice. Interestingly, the depletion of the $Sca1^{+}Thy1^{hi}$ cells in the TLR1-deficient RagKO mice had no effect on IL-23 or IL-12 (Fig. 8G).

To determine if any single cytokine was driving the heightened inflammation and the inability to heal in the 1KO mice, we administered either neutralizing antibodies to IFN-γ, IL-17, or IL-22 every other day for the seven-day course of DSS and weight loss and survival was measured. In line with other studies, there was moderate but significantly less weight loss in RagKO mice given DSS and treated with anti-IFN-γ (44) (Fig. 8G). In contrast, treatment with anti-IL-17 or anti-IL-22 resulted in much more weight loss (Fig. 8H and 8I, respectively) and a more severe histological disease in WT mice given DSS (data not shown). In the TLR1-deficient RagKO mice, anti-IFN-γ treatment resulted in a complete reversal of the observed weight loss, while anti-IL-17 and anti-IL-22 treatment had little effect on weight loss (Fig. 8H and 8I, respectively). Altogether, these data suggest that in the absence of TLR1 and under chronic inflammation, the $Sca1^{+}Thy1^{hi}$ cells shift produce IFN-γ, which is responsible for the worse pathology and severe disease observed following DSS.

DISCUSSION

Here, we show that endogenous TLR1 signaling is necessary to regulate homeostasis of the colon. In the absence of these TLR1 signals, there is a disruption of colonic crypt microarchitecture, mucosal-associated and translocated commensal bacteria and low level inflammation. The low-level inflammation was characterized by elevated IL-1β and IL-23 production and an increase in IL-22-producing $lin^{-}Sca1^{+}Thy1^{hi}RORC^{+}$ ILC3. Despite significantly more translocated bacteria, a leaky gut and heightened colonic inflammation, TLR1-deficient mice do not exhibit any overt phenotype. However, upon intestinal injury induced by DSS, TLR1-deficient mice decline rapidly and are unable to heal after DSS-withdrawal. Using neutralizing antibodies, we show that an increase in $Sca1^{+}Thy1^{hi}$ ILC3 and a concomitant rise in tissue levels of IFN-γ contribute to this phenotype.

One key question is whether the altered colonic epithelial phenotype of the 1KO is due to a primary impact of TLR1-deficiency, secondary to an altered microbiota and/or a response to chronic inflammation. TLR1KO mice had no major alterations in their cecal microbial community, and fecal microbiota transfer between 1KO and WT mice was not sufficient to induce inflammation arguing against a secondary effect due to a microbial dysbiosis. This is consistent with the work of Ubeda et al, who found only minor differences in microbial community when comparing littermates from TLR-deficient mouse strains (45). Bone marrow chimera studies determined that barrier function was mediated by TLR1 signaling in the non-hematopoietic cell compartment further suggesting that a defect of TLR1 in the epithelium is primary in this model. Whether epithelial derangement precedes the chronic inflammatory response or is a symptom of dysregulated immune activation is challenging to determine and these processes likely develop in concert *in vivo*.

The intestinal epithelium is in a state of constant renewal, being replaced roughly every 5 days (13, 35, 46) and this renewal is mediated via the coordinated signals of factors that are involved in proliferation and differentiation. In addition to the observation that TLR1-deficiency was associated with an increase in proliferation of the colonic crypt, we also found these mice had spatial and functional differences of the specialized epithelial cell. One intriguing finding was the presence of lysozyme- and α-defensin-1-expressing cells. These antimicrobial agents are typically restricted to the small intestine, where they are co-expressed in Paneth cells. Ectopic expression of Paneth cell markers has been reported in a number of studies (2, 6, 10, 37, 42, 47–49), particularly those examining WNT and Notch signaling due to their roles in proliferation (11, 46) and differentiation (50), respectively. However, we were unable to find any difference in *Notch-1* and its downstream target genes (unpublished observations).

There is increasing evidence that innate-sensing of the microbiota plays an important role in regulating epithelial cell proliferation. Studies using germ-free or antibiotic-treated mice have shown a reduction in the proliferation of IEC respective to controls (12, 51–53). More recently, a comparison of antibiotics that favor either the depletion of gram-positive or gram-negative bacteria found a reduction in proliferation when only the gram-positive bacteria were depleted (11). However, the data concerning the role of MyD88 in this process are conflicting. Using MyD88KO mice, Rakouf-Nahoum et al reported that commensal TLR signaling was required for homeostasis and, in particular, found an increase in the number of BrdU+ cells in the colons of MyD88KO mice, suggesting an inhibitory role of TLRs on proliferation (7), yet subsequent reports have demonstrated that TLR and MyD88 signaling promote epithelial proliferation (5, 11, 14). Our data aligns with the studies by Rakoff-Nahoum, as we identified a significant increase in Brdu+ and Ki67+ cells within the colonic epithelium of naïve TLR1-deficient mice. An intriguing possibility is that engagement of commensal-derived TLR1 ligands may induce a genetic program that regulates or coordinates signaling of growth and/or differentiation factors in the colon leading to regulation of proliferation. However, analysis of *Notch1, Wnt5a, Wnt3, Jagged1*, and the downstream Notch1-responsive transcription factor *Hes1*, revealed no difference in expression between the colons of WT and 1KO mice (Supplemental Fig. 2 and unpublished data). The Notch and WNT families contain many members and are both regulated by a variety of different factors. Thus, a much more comprehensive screen looking at the role of

TLR1 in the direct regulation of WNT and Notch family members and their inhibitors is currently underway in our laboratory.

Here, using antibiotics to deplete the commensal microbiota, we provide evidence that the microbiota is necessary for the increased proliferation observed in the TLR1-deficient mice, yet the composition and the function of the microbiota from TLR1-deficient mice were not sufficient to induce this proliferative response when transferred to antibiotic-treated WT recipients. These data do not exclude a role for TLR1 in directly regulating the growth and differentiation signals in the crypt, as it is possible that through other innate immune receptors the microbiome drives proliferation and TLR1 drives regulatory factors that counter this commensal-driven activation.

Our study is also the first to identify a role of TLR1 in regulation of the epithelium and the first to support a regulatory role for this molecule in proliferation. Our data is in sharp contrast to studies using TLR2 agonists (25, 26) and TLR2KO mice (5, 11, 14), which show increased and decreased proliferation, respectively. TLR1 forms a heterodimer with TLR2 to recognize tri-acylated lipoproteins (11, 12, 28) (28). Our group, and others, have shown that TLR2/1 signaling induces pro-inflammatory innate immune responses through activation of MyD88 and NFkB or Pi3K/Akt and mTOR (3, 22, 23, 34, 38, 54, 55) in immune cells, but its downstream signaling pathways may be different in epithelial cells due to the expression of different co-receptors. The promiscuity in binding by TLR2 allows it to form complexes with co-receptors TLR6, TLR10, Dectin-1, TLR4, CD14 and CD36. Analysis of mRNA transcripts for *Tlr1* by our group has revealed increasing expression as you move distally from the ileum to the rectum. In porcine small intestinal tissue, *Tlr1* gene expression is low at the base of the crypt and increases as you move towards the villous tip (56). *Tlr1* expression has also been observed in the colons of naïve mice, yet unlike expression of *Tlr2* and *Tlr6* which increases during DSS administration, *Tlr1* expression remains unchanged (57). Additionally, it is not known whether TLR1, TLR6 and TLR10 compete with each other for binding with TLR2, as no studies to date have analyzed TLR2/6 and TLR2/10 expression in 1KO mice or in individuals with the polymorphisms that disrupt cellular surface expression, such as the TLR1 I602S polymorphism. It is a distinct possibility that shifting recognition of commensal ligands to TLR2/6 or, in humans, TLR2/10, may promote proliferation. Interestingly, analysis of TLR6-deficient crypts revealed no change in the number of BrdU+ cells (unpublished observations) further demonstrating the differential effects mediated by TLR1 and TLR6.

We observed a shift in the expression of cytokines and transcription factors in the lin^{-}Sca1^{+}Thy1^{hi} ILC3 in the TLR1-deficient mice. In naive WT and 1KO controls these cells expressed higher levels of *Il22* but the latter also expressed transcripts for *Il17*. Upon tissue injury induced by DSS, the lin^{-}Sca1^{+}Thy1^{hi} cells from WT mice had an increase in *Il22* transcripts as well as *Il17*. In contrast, after DSS induced injury in the 1KO there was an increase in *Tbet* and *Ifng* expression in the lin^{-}Sca1^{+}Thy1^{hi} cells (data not shown) that correlated with an elevation of IFN-γ protein in the tissue. This phenotype, along with our observed increase in IL-12, is reminiscent of IL-22^{+}Rorγt^{+} ILC3, which acquire *Tbet* in the presence of IL-12 and have been termed “exILC3” in both mice and humans (8, 58). It is well established that IFN-γ negatively regulates the epithelial barrier and antagonizes

proliferation (15, 59, 60) and thus its presence during DSS in the 1KO mice would block the beneficial effects of IL-22, thereby preventing epithelial proliferation and exacerbating the damage. Indeed, depletion of the $Thy1^+$ cells in the TLR1-deficient RagKO mice and neutralization of IFN-γ both ameliorated the severity of DSS administration. Other studies have shown that chronic inflammation of the intestine leads to IL-12 production and the expansion of IFN-γ^+ cells (48, 49, 61) or the re-programming of IL-17 expressing cells (36).

Our results provide new insight into the regulation of the colonic crypt and suggest an unexpected role for TLR1-sensing of endogenous ligands in this process. Understanding how the microbiome may contribute to epithelial homeostasis and the consequence of disrupted signaling through host genes or changes in the gut microbiome has broad implications. These data provide biological evidence for the observations of an increased frequency of patients expressing mutations in the TLR1 locus with IBD, and that IBD patients expressing defective TLR1 genes are more likely to have anti-commensal antibodies (18, 54). These studies also provide a biological framework for the development of TLR1 agonists that could be used to promote a healthy intestinal barrier and suggests that persons expressing variant *TLR1* alleles may be at a higher risk for developing systemic inflammation, leaky gut and long term chronic intestinal disease.

Supplementary Material

Refer to Web version on PubMed Central for supplementary material.

Acknowledgments

We'd like to thank Denise Chac for her assistance in editing the paper.

This work was supported by NIH R01 DK104908-01 (RWD).

References

1. Abreu MT. 2010; Toll-like receptor signalling in the intestinal epithelium: how bacterial recognition shapes intestinal function. Nat Rev Immunol. 10:131–144. [PubMed: 20098461]
2. Andreu P, Colnot S, Godard C, Gad S, Chafey P, Niwa-Kawakita M, Laurent-Puig P, Kahn A, Robine S, Perret C, Romagnolo B. 2005; Crypt-restricted proliferation and commitment to the Paneth cell lineage following Apc loss in the mouse intestine. Development. 132:1443–1451. [PubMed: 15716339]
3. Garrett WS, Gordon JI, Glimcher LH. 2010; Homeostasis and inflammation in the intestine. Cell. 140:859–870. [PubMed: 20303876]
4. Tremaroli V, Backhed F. 2012; Functional interactions between the gut microbiota and host metabolism. Nature. 489:242–249. [PubMed: 22972297]
5. Behrens J. 2000; Control of beta-catenin signaling in tumor development. Ann N Y Acad Sci. 910:21–33. [PubMed: 10911903]
6. Andreu P, Peignon G, Slomianny C, Taketo MM, Colnot S, Robine S, Lamarque D, Laurent-Puig P, Perret C, Romagnolo B. 2008; A genetic study of the role of the Wnt/beta-catenin signalling in Paneth cell differentiation. Dev Biol. 324:288–296. [PubMed: 18948094]
7. Rakoff-Nahoum S, Paglino J, Eslami-Varzaneh F, Edberg S, Medzhitov R. 2004; Recognition of commensal microflora by toll-like receptors is required for intestinal homeostasis. Cell. 118:229–241. [PubMed: 15260992]
8. Bernink JH, Peters CP, Munneke M, te Velde AA, Meijer SL, Weijer K, Hreggvidsdottir HS, Heinsbroek SE, Legrand N, Buskens CJ, Bemelman WA, Mjosberg JM, Spits H. 2013; Human type

1 innate lymphoid cells accumulate in inflamed mucosal tissues. Nat Immunol. 14:221–229. [PubMed: 23334791]

9. Barman M, Unold D, Shifley K, Amir E, Hung K, Bos N, Salzman N. 2008; Enteric salmonellosis disrupts the microbial ecology of the murine gastrointestinal tract. Infect Immun. 76:907–915. [PubMed: 18160481]
10. Kufer TA, Sansonetti PJ. 2011; NLR functions beyond pathogen recognition. Nat Immunol. 12:121–128. [PubMed: 21245903]
11. Park JH, Kotani T, Konno T, Setiawan J, Kitamura Y, Imada S, Usui Y, Hatano N, Shinohara M, Saito Y, Murata Y, Matozaki T. 2016; Promotion of Intestinal Epithelial Cell Turnover by Commensal Bacteria: Role of Short-Chain Fatty Acids. PLoS One. 11:e0156334. [PubMed: 27232601]
12. Reikvam DH, Erofeev A, Sandvik A, Grcic V, Jahnsen FL, Gaustad P, McCoy KD, Macpherson AJ, Meza-Zepeda LA, Johansen FE. 2011; Depletion of murine intestinal microbiota: effects on gut mucosa and epithelial gene expression. PLoS One. 6:e17996. [PubMed: 21445311]
13. Khoury KA, Floch MH, Hersh T. 1969; Small intestinal mucosal cell proliferation and bacterial flora in the conventionalization of the germfree mouse. J Exp Med. 130:659–670. [PubMed: 4896909]
14. Bogunovic M, Dave SH, Tilstra JS, Chang DT, Harpaz N, Xiong H, Mayer LF, Plevy SE. 2007; Enteroendocrine cells express functional Toll-like receptors. Am J Physiol Gastrointest Liver Physiol. 292:G1770–1783. [PubMed: 17395901]
15. Bruewer M, Samarin S, Nusrat A. 2006; Inflammatory bowel disease and the apical junctional complex. Ann N Y Acad Sci. 1072:242–252. [PubMed: 17057204]
16. Buonocore S, Ahern PP, Uhlig HH, Ivanov, Littman DR, Maloy KJ, Powrie F. 2010; Innate lymphoid cells drive interleukin-23-dependent innate intestinal pathology. Nature. 464:1371–1375. [PubMed: 20393462]
17. Cario E, Gerken G, Podolsky DK. 2004; Toll-like receptor 2 enhances ZO-1-associated intestinal epithelial barrier integrity via protein kinase C. Gastroenterology. 127:224–238. [PubMed: 15236188]
18. Kamdar K, Khakpour S, Chen J, Leone V, Brulc J, Mangatu T, Antonopoulos DA, Chang EB, Kahn SA, Kirschner BS, Young G, DePaolo RW. 2016; Genetic and Metabolic Signals during Acute Enteric Bacterial Infection Alter the Microbiota and Drive Progression to Chronic Inflammatory Disease. Cell Host Microbe. 19:21–31. [PubMed: 26764594]
19. Cua DJ, Sherlock J, Chen Y, Murphy CA, Joyce B, Seymour B, Lucian L, To W, Kwan S, Churakova T, Zurawski S, Wiekowski M, Lira SA, Gorman D, Kastelein RA, Sedgwick JD. 2003; Interleukin-23 rather than interleukin-12 is the critical cytokine for autoimmune inflammation of the brain. Nature. 421:744–748. [PubMed: 12610626]
20. Gong J, Xu J, Zhu W, Gao X, Li N, Li J. 2010; Epithelial-specific blockade of MyD88-dependent pathway causes spontaneous small intestinal inflammation. Clin Immunol. 136:245–256. [PubMed: 20452828]
21. Hisamatsu T, Suzuki M, Reinecker HC, Nadeau WJ, McCormick BA, Podolsky DK. 2003; CARD15/NOD2 functions as an antibacterial factor in human intestinal epithelial cells. Gastroenterology. 124:993–1000. [PubMed: 12671896]
22. DePaolo RW, Kamdar K, Khakpour S, Sugiura Y, Wang W, Jabri B. 2012; A specific role for TLR1 in protective T(H)17 immunity during mucosal infection. J Exp Med. 209:1437–1444. [PubMed: 22778390]
23. Depaolo RW, Tang F, Kim I, Han M, Levin N, Ciletti N, Lin A, Anderson D, Schneewind O, Jabri B. 2008; Toll-like receptor 6 drives differentiation of tolerogenic dendritic cells and contributes to LcrV-mediated plague pathogenesis. Cell Host Microbe. 4:350–361. [PubMed: 18854239]
24. Yamamoto M, Sato S, Hemmi H, Hoshino K, Kaisho T, Sanjo H, Takeuchi O, Sugiyama M, Okabe M, Takeda K, Akira S. 2003; Role of adaptor TRIF in the MyD88-independent toll-like receptor signaling pathway. Science. 301:640–643. [PubMed: 12855817]
25. Dessein R, Gironella M, Vignal C, Peyrin-Biroulet L, Sokol H, Secher T, Lacas-Gervais S, Gratadoux JJ, Lafont F, Dagorn JC, Ryffel B, Akira S, Langella P, Nunez G, Sirard JC, Iovanna J, Simonet M, Chamaillard M. 2009; Toll-like receptor 2 is critical for induction of Reg3 beta

expression and intestinal clearance of Yersinia pseudotuberculosis. Gut. 58:771–776. [PubMed: 19174417]

26. Hormann N, Brandao I, Jackel S, Ens N, Lillich M, Walter U, Reinhardt C. 2014; Gut microbial colonization orchestrates TLR2 expression, signaling and epithelial proliferation in the small intestinal mucosa. PLoS One. 9:e113080. [PubMed: 25396415]
27. Eberl G. 2012; Development and evolution of RORgammat+ cells in a microbe's world. Immunol Rev. 245:177–188. [PubMed: 22168420]
28. Farhat K, Riekenberg S, Heine H, Debarry J, Lang R, Mages J, Buwitt-Beckmann U, Roschmann K, Jung G, Wiesmuller KH, Ulmer AJ. 2008; Heterodimerization of TLR2 with TLR1 or TLR6 expands the ligand spectrum but does not lead to differential signaling. J Leukoc Biol. 83:692–701. [PubMed: 18056480]
29. Birchenough GM, Nystrom EE, Johansson ME, Hansson GC. 2016; A sentinel goblet cell guards the colonic crypt by triggering Nlrp6-dependent Muc2 secretion. Science. 352:1535–1542. [PubMed: 27339979]
30. Johansson ME, Hansson GC. 2016; Immunological aspects of intestinal mucus and mucins. Nat Rev Immunol. 16:639–649. [PubMed: 27498766]
31. Winter SE, Thiennimitr P, Winter MG, Butler BP, Huseby DL, Crawford RW, Russell JM, Bevins CL, Adams LG, Tsolis RM, Roth JR, Baumler AJ. 2010; Gut inflammation provides a respiratory electron acceptor for Salmonella. Nature. 467:426–429. [PubMed: 20864996]
32. Caporaso JG, Lauber CL, Walters WA, Berg-Lyons D, Lozupone CA, Turnbaugh PJ, Fierer N, Knight R. 2011; Global patterns of 16S rRNA diversity at a depth of millions of sequences per sample. Proc Natl Acad Sci U S A. 108(Suppl 1):4516–4522. [PubMed: 20534432]
33. Kozich JJ, Westcott SL, Baxter NT, Highlander SK, Schloss PD. 2013; Development of a dual-index sequencing strategy and curation pipeline for analyzing amplicon sequence data on the MiSeq Illumina sequencing platform. Appl Environ Microbiol. 79:5112–5120. [PubMed: 23793624]
34. Sugiura Y, Kamdar K, Khakpour S, Young G, Karpus WJ, DePaolo RW. 2013; TLR1-induced chemokine production is critical for mucosal immunity against Yersinia enterocolitica. Mucosal Immunol. 6:1101–1109. [PubMed: 23443468]
35. Guo X, Qiu J, Tu T, Yang X, Deng L, Anders RA, Zhou L, Fu YX. 2014; Induction of innate lymphoid cell-derived interleukin-22 by the transcription factor STAT3 mediates protection against intestinal infection. Immunity. 40:25–39. [PubMed: 24412612]
36. Harbour SN, Maynard CL, Zindl CL, Schoeb TR, Weaver CT. 2015; Th17 cells give rise to Th1 cells that are required for the pathogenesis of colitis. Proc Natl Acad Sci U S A. 112:7061–7066. [PubMed: 26038559]
37. Hirata A, Utikal J, Yamashita S, Aoki H, Watanabe A, Yamamoto T, Okano H, Bardeesy N, Kunisada T, Ushijima T, Hara A, Jaenisch R, Hochedlinger K, Yamada Y. 2013; Dose-dependent roles for canonical Wnt signalling in de novo crypt formation and cell cycle properties of the colonic epithelium. Development. 140:66–75. [PubMed: 23222438]
38. Petermann F, Rothhammer V, Claussen MC, Haas JD, Blanco LR, Heink S, Prinz I, Hemmer B, Kuchroo VK, Oukka M, Korn T. 2010; gammadelta T cells enhance autoimmunity by restraining regulatory T cell responses via an interleukin-23-dependent mechanism. Immunity. 33:351–363. [PubMed: 20832339]
39. Takatori H, Kanno Y, Watford WT, Tato CM, Weiss G, Ivanov, Littman DR, O'Shea JJ. 2009; Lymphoid tissue inducer-like cells are an innate source of IL-17 and IL-22. J Exp Med. 206:35–41. [PubMed: 19114665]
40. Wlodarska M, Thaiss CA, Nowarski R, Henao-Mejia J, Zhang JP, Brown EM, Frankel G, Levy M, Katz MN, Philbrick WM, Elinav E, Finlay BB, Flavell RA. 2014; NLRP6 inflammasome orchestrates the colonic host-microbial interface by regulating goblet cell mucus secretion. Cell. 156:1045–1059. [PubMed: 24581500]
41. Keshav S. 2006; Paneth cells: leukocyte-like mediators of innate immunity in the intestine. J Leukoc Biol. 80:500–508. [PubMed: 16793911]
42. Ouellette AJ. 2010; Paneth cells and innate mucosal immunity. Curr Opin Gastroenterol. 26:547–553. [PubMed: 20693892]

43. Steenwinckel V, Louahed J, Lemaire MM, Sommereyns C, Warnier G, McKenzie A, Brombacher F, Van Snick J, Renauld JC. 2009; IL-9 promotes IL-13-dependent paneth cell hyperplasia and up-regulation of innate immunity mediators in intestinal mucosa. J Immunol. 182:4737–4743. [PubMed: 19342650]
44. Ito R, Shin-Ya M, Kishida T, Urano A, Takada R, Sakagami J, Imanishi J, Kita M, Ueda Y, Iwakura Y, Kataoka K, Okanoue T, Mazda O. 2006; Interferon-gamma is causatively involved in experimental inflammatory bowel disease in mice. Clin Exp Immunol. 146:330–338. [PubMed: 17034586]
45. Ubeda C, Lipuma L, Gobourne A, Viale A, Leiner I, Equinda M, Khanin R, Pamer EG. 2012; Familial transmission rather than defective innate immunity shapes the distinct intestinal microbiota of TLR-deficient mice. J Exp Med. 209:1445–1456. [PubMed: 22826298]
46. Krausova M, Korinek V. 2014; Wnt signaling in adult intestinal stem cells and cancer. Cell Signal. 26:570–579. [PubMed: 24308963]
47. Feng Y, Sentani K, Wiese A, Sands E, Green M, Bommer GT, Cho KR, Fearon ER. 2013; Sox9 induction, ectopic Paneth cells, and mitotic spindle axis defects in mouse colon adenomatous epithelium arising from conditional biallelic Apc inactivation. Am J Pathol. 183:493–503. [PubMed: 23769888]
48. Matsuoka K, Inoue N, Sato T, Okamoto S, Hisamatsu T, Kishi Y, Sakuraba A, Hitotsumatsu O, Ogata H, Koganei K, Fukushima T, Kanai T, Watanabe M, Ishii H, Hibi T. 2004; T-bet upregulation and subsequent interleukin 12 stimulation are essential for induction of Th1 mediated immunopathology in Crohn's disease. Gut. 53:1303–1308. [PubMed: 15306590]
49. Neurath MF, Weigmann B, Finotto S, Glickman J, Nieuwenhuis E, Iijima H, Mizoguchi A, Mizoguchi E, Mudter J, Galle PR, Bhan A, Autschbach F, Sullivan BM, Szabo SJ, Glimcher LH, Blumberg RS. 2002; The transcription factor T-bet regulates mucosal T cell activation in experimental colitis and Crohn's disease. J Exp Med. 195:1129–1143. [PubMed: 11994418]
50. VanDussen KL, Carulli AJ, Keeley TM, Patel SR, Puthoff BJ, Magness ST, Tran IT, Maillard I, Siebel C, Kolterud A, Grosse AS, Gumucio DL, Ernst SA, Tsai YH, Dempsey PJ, Samuelson LC. 2012; Notch signaling modulates proliferation and differentiation of intestinal crypt base columnar stem cells. Development. 139:488–497. [PubMed: 22190634]
51. Scoville DH, Sato T, He XC, Li L. 2008; Current view: intestinal stem cells and signaling. Gastroenterology. 134:849–864. [PubMed: 18325394]
52. Smith K, McCoy KD, Macpherson AJ. 2007; Use of axenic animals in studying the adaptation of mammals to their commensal intestinal microbiota. Semin Immunol. 19:59–69. [PubMed: 17118672]
53. Pull SL, Doherty JM, Mills JC, Gordon JI, Stappenbeck TS. 2005; Activated macrophages are an adaptive element of the colonic epithelial progenitor niche necessary for regenerative responses to injury. Proc Natl Acad Sci U S A. 102:99–104. [PubMed: 15615857]
54. Pierik M, Joossens S, Van Steen K, Van Schuerbeek N, Vlietinck R, Rutgeerts P, Vermeire S. 2006; Toll-like receptor-1, -2, and -6 polymorphisms influence disease extension in inflammatory bowel diseases. Inflamm Bowel Dis. 12:1–8. [PubMed: 16374251]
55. Santos-Sierra S, Deshmukh SD, Kalnitski J, Kuenzi P, Wymann MP, Golenbock DT, Henneke P. 2009; Mal connects TLR2 to PI3Kinase activation and phagocyte polarization. EMBO J. 28:2018–2027. [PubMed: 19574958]
56. Gourbeyre P, Berri M, Lippi Y, Meurens F, Vincent-Naulleau S, Laffitte J, Rogel-Gaillard C, Pinton P, Oswald IP. 2015; Pattern recognition receptors in the gut: analysis of their expression along the intestinal tract and the crypt/villus axis. Physiol Rep. 3
57. Zheng B, Morgan ME, van de Kant HJ, Garssen J, Folkerts G, Kraneveld AD. 2013; Transcriptional modulation of pattern recognition receptors in acute colitis in mice. Biochim Biophys Acta. 1832:2162–2172. [PubMed: 23851050]
58. Vonarbourg C, Mortha A, Bui VL, Hernandez PP, Kiss EA, Hoyler T, Flach M, Bengsch B, Thimme R, Holscher C, Honig M, Pannicke U, Schwarz K, Ware CF, Finke D, Diefenbach A. 2010; Regulated expression of nuclear receptor RORgammat confers distinct functional fates to NK cell receptor-expressing RORgammat(+) innate lymphocytes. Immunity. 33:736–751. [PubMed: 21093318]

59. Kaiser GC, Polk DB. 1997; Tumor necrosis factor alpha regulates proliferation in a mouse intestinal cell line. Gastroenterology. 112:1231–1240. [PubMed: 9098007]

60. Ruemmele FM, Gurbindo C, Mansour AM, Marchand R, Levy E, Seidman EG. 1998; Effects of interferon gamma on growth, apoptosis, and MHC class II expression of immature rat intestinal crypt (IEC-6) cells. J Cell Physiol. 176:120–126. [PubMed: 9618152]

61. Fuss IJ, Becker C, Yang Z, Groden C, Hornung RL, Heller F, Neurath MF, Strober W, Mannon PJ. 2006; Both IL-12p70 and IL-23 are synthesized during active Crohn's disease and are down-regulated by treatment with anti-IL-12 p40 monoclonal antibody. Inflamm Bowel Dis. 12:9–15. [PubMed: 16374252]

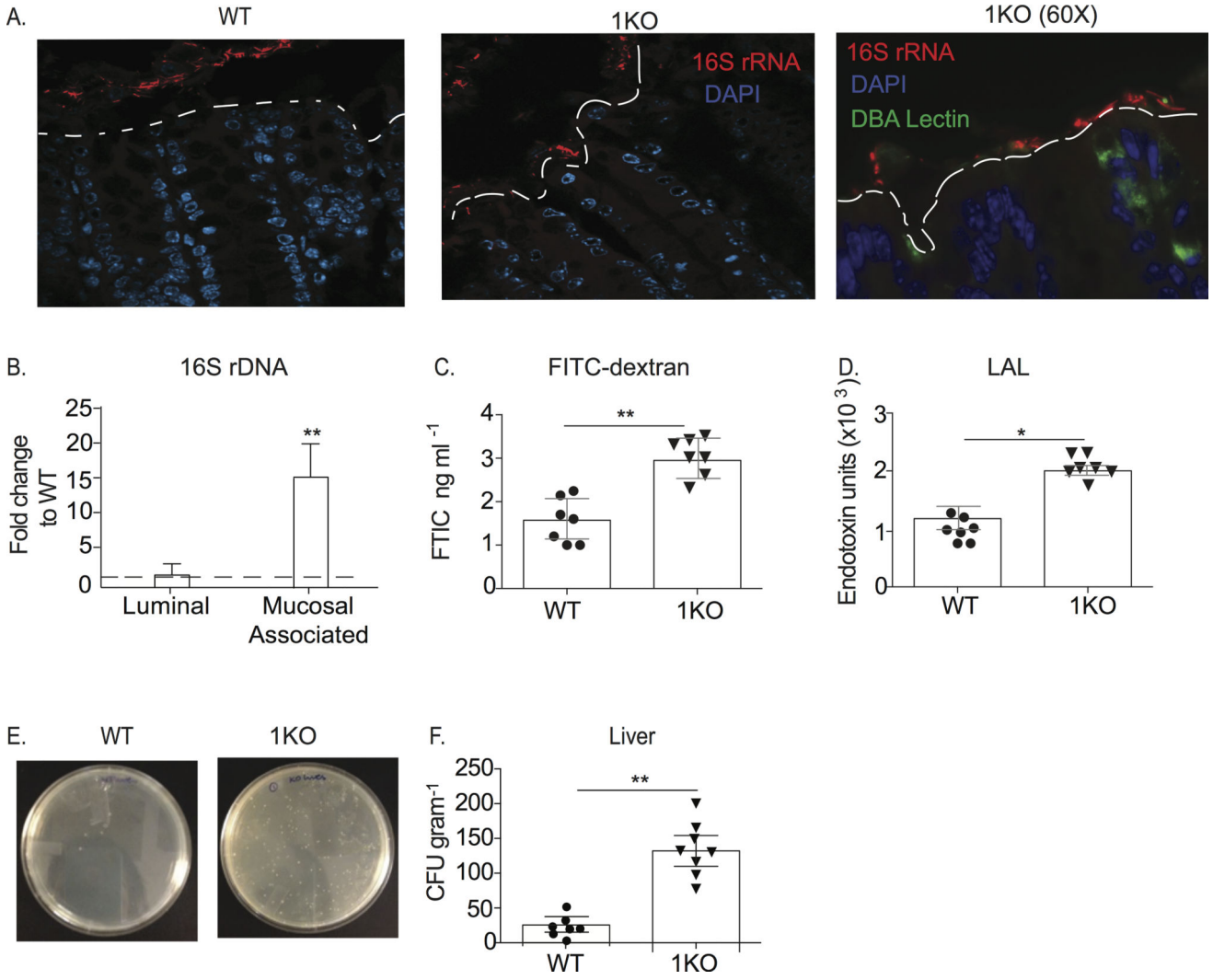

Figure 1. Expression of TLR1 prevents mucosal-associated bacteria and their translocation to the periphery

Colons from naïve 1KO mice were compared to naïve WT colons. (A) Representative 40X confocal images from Carnoy's fixed sections of the distal colon of WT and 1KO mice hybridized with a probe against eubacterial 16S rRNA (red) and counter stained with DAPI (blue). Image on far right is a fluorescent microscope image of 1KO with using the 16S FISH probe (red), DAPI (blue) and DBA lectin (green). (B) Fold change of 16S DNA expression from 1KO luminal colonic contents or colonic mucosal scrapings normalized to WT. (C) Relative fluorescent units in the serum of WT and 1KO mice 1 hour post-intrarectal administration of FITC-Dextran. Each dot represents an individual mouse. (D) Endotoxin units from serum of WT and 1KO mice as determined using LAL test. Each dot represents an individual mouse. (E) Representative bacterial plates from livers of 1KO and WT mice. (F) CFU per gram of liver cultured anaerobically on TSA plates. Each dot represents an individual mouse. (Data is represented as the mean ± s.e.m from 2–3independent experiments. A, n= 3 mice per group; B–F, n= 7–10 mice per group; *, $p<0.05$, **, $p<0.01$. Student's unpaired t-test.

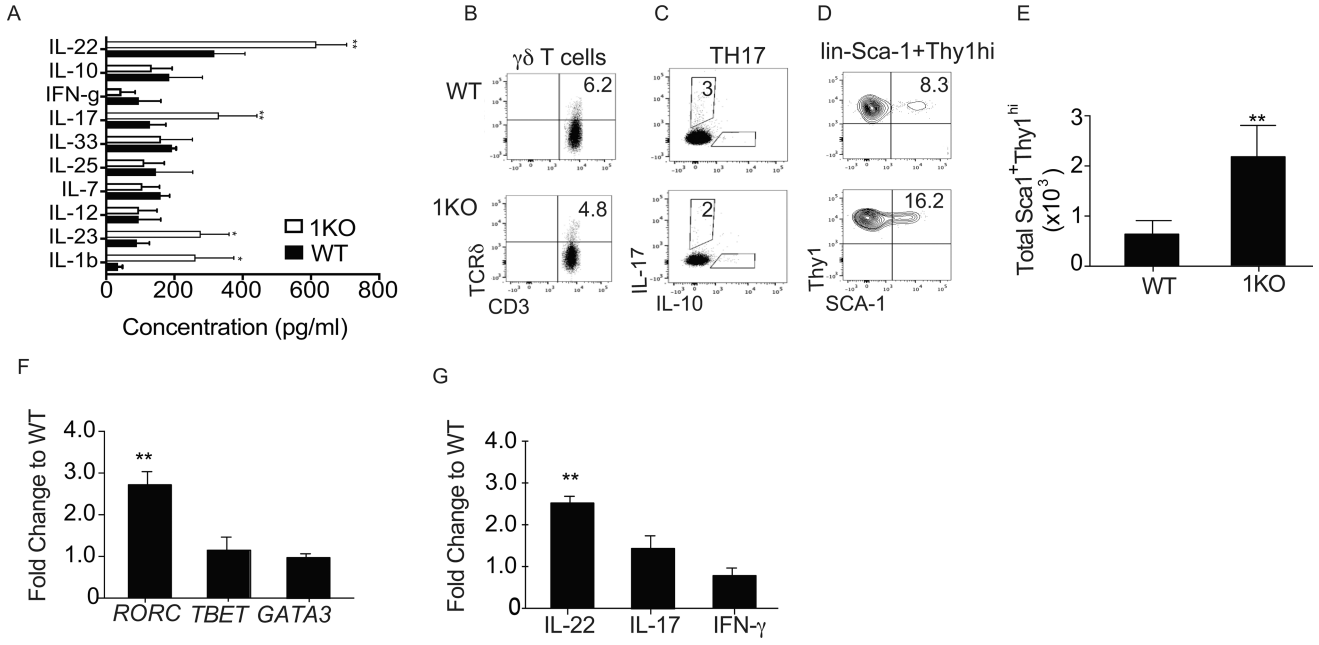

Figure 2. TLR1-deficiency is associated with disturbed immune homeostasis in the colonic lamina propria

(A) Cytokine levels in whole colonic lysate were measured and normalized to the weight of the tissue of naive 1KO and WT. Representative FACS plots of naïve WT and 1KO lamina propria cells. Dead cells were excluded and all live cells were gated on FSC and SSC, (B) CD3+ and TCR δ+ T cells, (C) CD3+CD4+ and intracellular IL-17 and IL-10 and (D) lin^- ($CD11b^-$, $CD11c^-$, $NKp44^-$, $F480^-$, $B220^-$, $CD19^-$, $CD3^-$), $Sca1^+$ and $Thy1^{hi}$ cells. Relative expression of mRNA transcripts for indicated (E) Absolute cell number of lin-Sca1+Thy1hi cells in the colonic lamina propria from mice. $lin^-Sca1^+Thy1^{hi}$ cells were sorted from the colonic lamina propria and quantitative RT-PCR was performed to obtain relative expression levels of (F) transcription factors and (G) cytokines using GAPDH as a reference housekeeping gene and showing fold changed to WT using $2^{-\Delta\Delta ct}$. Data is pooled from 2 independent experiments; A, E–G is expressed as mean ± s.e.m. A–E n=5–6 mice per group. F–G, Cells were isolated by pooling isolated and sorted $lin^-Sca1^+Thy1^{hi}$ from two mice from each genotype and the experiment was repeated twice. *, $p<0.05$, **, $p<0.01$, ***, $p<0.001$. A, One-way ANOVA, E–G, Student's unpaired t-test.

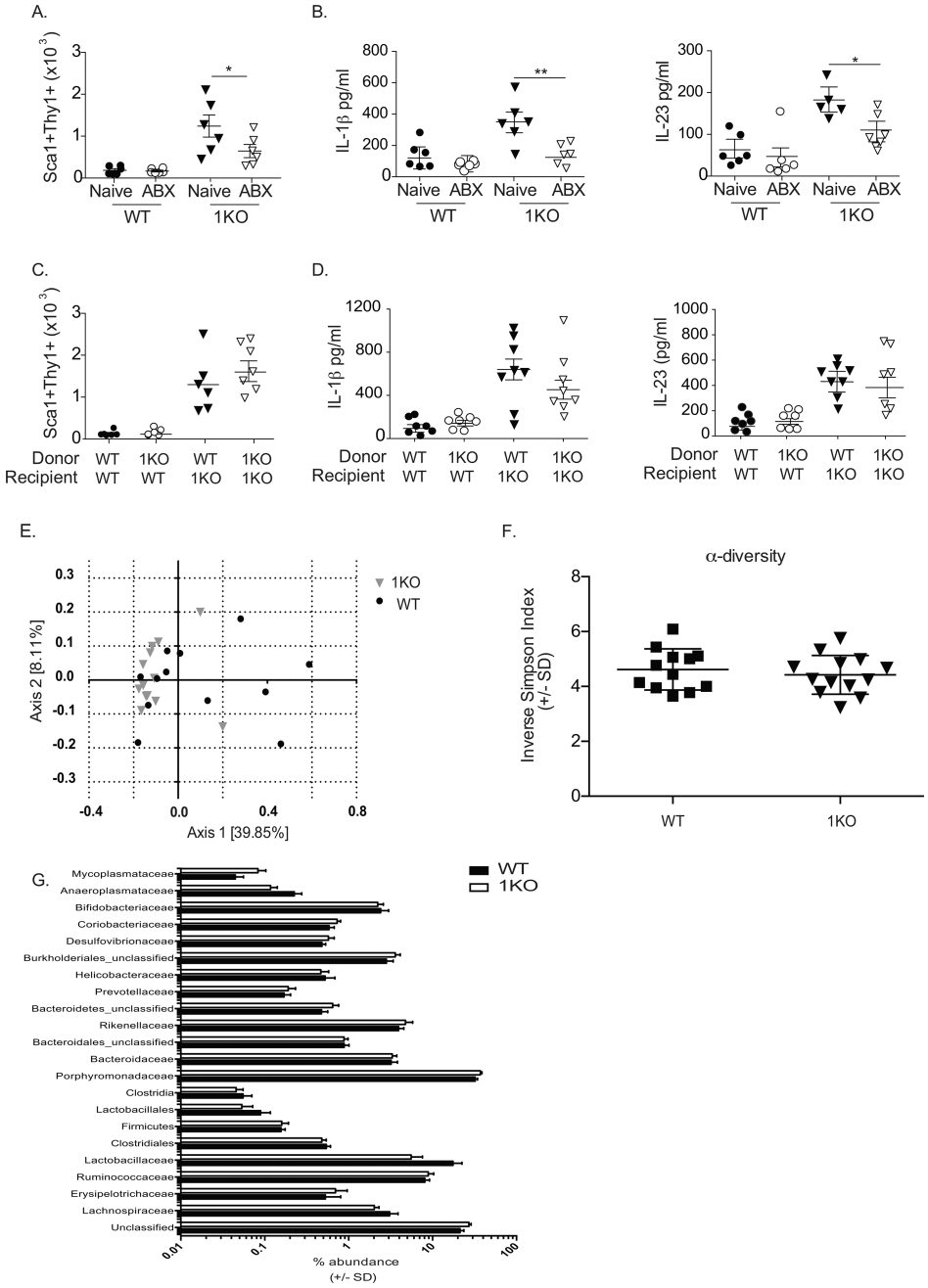

Figure 3. The microbiota of the 1KO mice is required for homeostatic immune regulation

(A–B) 1KO and WT mice born from antibiotic treated pregnant dams were maintained on antibiotic-treated water 1–2 weeks after weaning and analyzed for (A) absolute number of $lin^{-}Sca1^{+}Thy1^{hi}$ cells in antibiotic treated WT and 1KO mice compared to naïve (untreated) mice determined by flow cytometry, and (B) the concentration of IL-1ß and IL-23 detected in colonic homogenates as measured by ELISA. (C–D) A different set of antibiotic-treated WT and 1KO mice were given a fecal microbiota transplant (FMT) from the indicated donors and allowed to reconstitute for two weeks before quantification of (C) absolute cell number of lin-Sca1+Thy1hi cells and (D) concentration of IL-1ß and IL-23 detected in the

colonic lamina propria of FMT-treated WT and 1KO mice. Data is expressed individual mice pooled from 2–3 independent experiments with A–B, n=5–6 mice per group; C–D, n=5–9 mice per group. *, $p<0.05$, **, $p<0.01$. One-way ANOVA. E) PCoA analysis based on genus level identification of 16s rDNA sequences from 1KO (n = 13) or WT (n = 12) mouse cecal contents. F) Inverse-Simpson measurement of α-diversity in 1KO and WT mice. G) Family relative abundance in 1KO and WT cecal contents. Student's t test with false discovery rate correction showed no significant difference in relative abundance of different families between 1KO and WT mice.

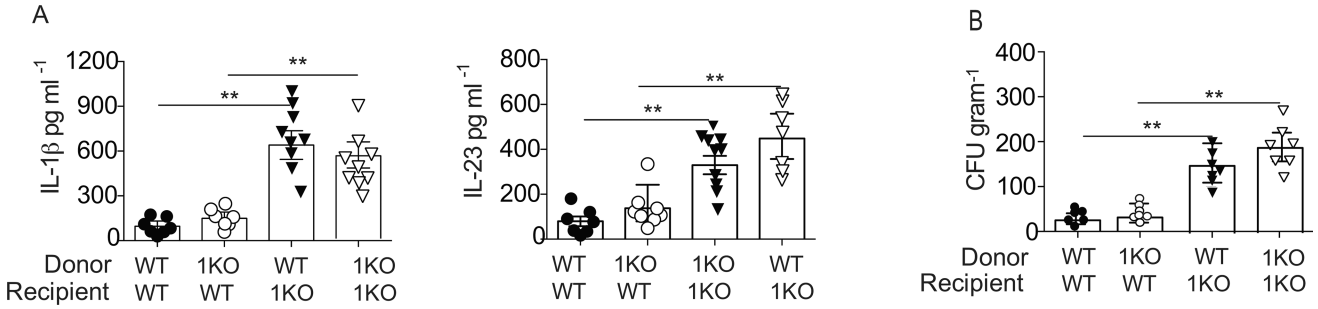

Figure 4. Aberrant immune activation is due to loss of TLR1 signaling in the epithelium

Bone marrow chimeras were generated using WT and 1KO recipients and WT and 1KO mice as donors. Six weeks after reconstitution (A) IL-1β and IL-23 levels from the colonic lamina propria were measured and (B) the number of bacteria in the liver was evaluated by qPCR for 16S. A–B, data is represented as the mean ± s.e.m. from two independent experiments with n= 7–9 mice per group. *, $p<0.05$, **, $p<0.01$. One-way ANOVA.

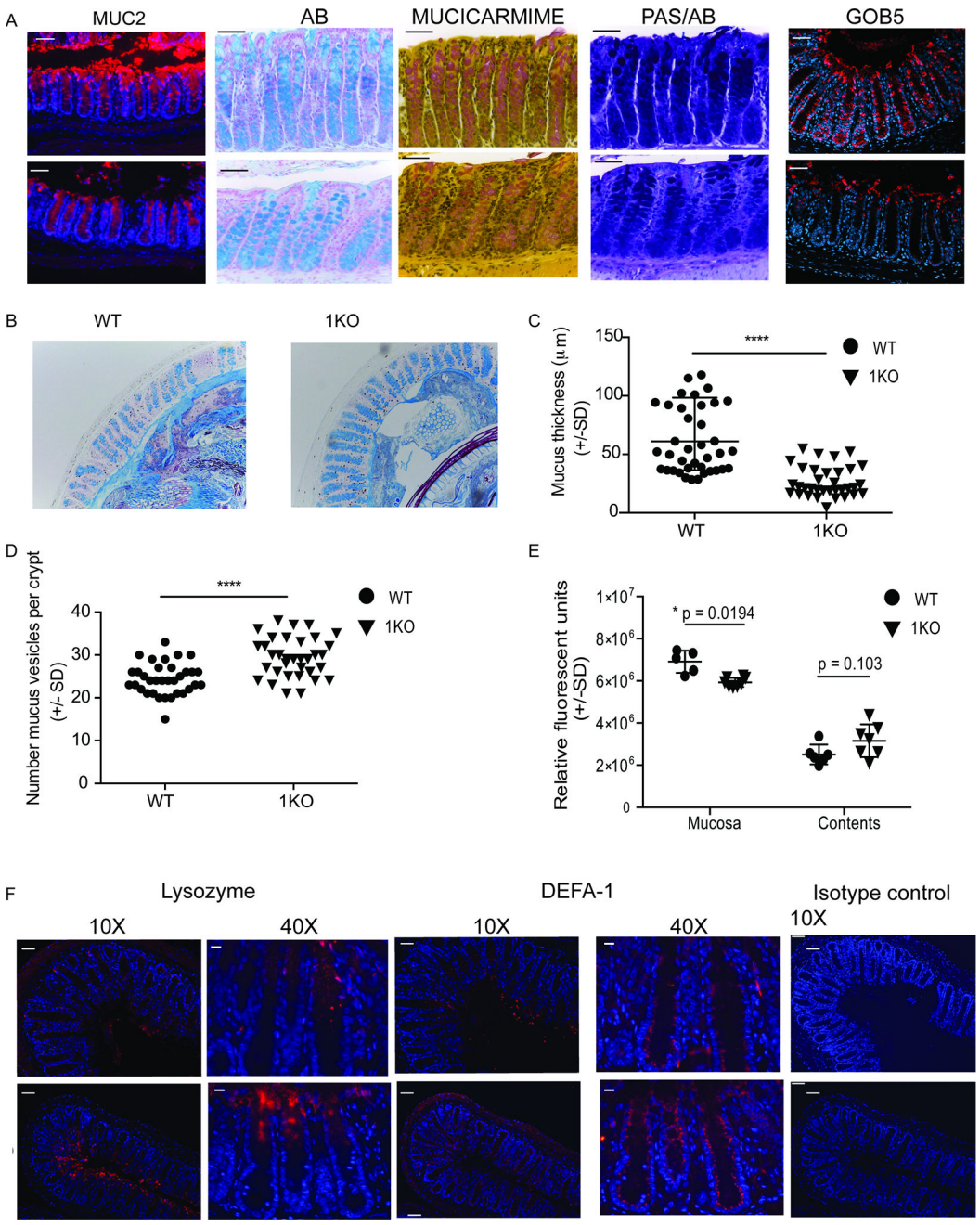

Figure 5. Reduced mucus secretion and an increase in anti-bacterial peptides occurs in the colonic crypt in the absence of TLR1 signaling

Methacarn-fixed sections from the colons of WT and 1KO mice were stained by immunohistochemistry for the indicated markers. (A) 40X fluorescent microscopy images of colon tissue stained for MUC2 (peptide sequence of mucin), Alcian blue (AB)(acidic mucins), Mucicarmine (acidic mucins) and Periodic Acid Schiff and Alcian Blue (PAS/AB) (neutral/acidic mucins). Scale bar equals 50 microns. Confocal images of GOB5 (mCLCA3) staining of the distal colon. (B) Alcian blue stained distal colonic sections from WT and 1KO mice were used for quantification of (C) mucus layer thickness and (D) Alcian blue positive vesicles per crypt. (E) Relative ROS activity in mucosa and colonic contents. (F)

10X and 40X fluorescent microscope images of distal colon stained with antibodies against lysozyme and a-defensin-1 (DEFA-1) and 10X image of isotype control. Scale bar equals 50 microns. A–B and F, representative images taken from 3–5 mice per group; C and D, individual measurements of mucus thickness along the distal colon taken from 3 mice per group; E, each point is an individual mouse from two different experiments. C and D, ****, $p<0.0001$ Mann-Whitney Test; F, *, $p = 0.02$ Students' t-test corrected for multiple comparisons (Holm-Sidak

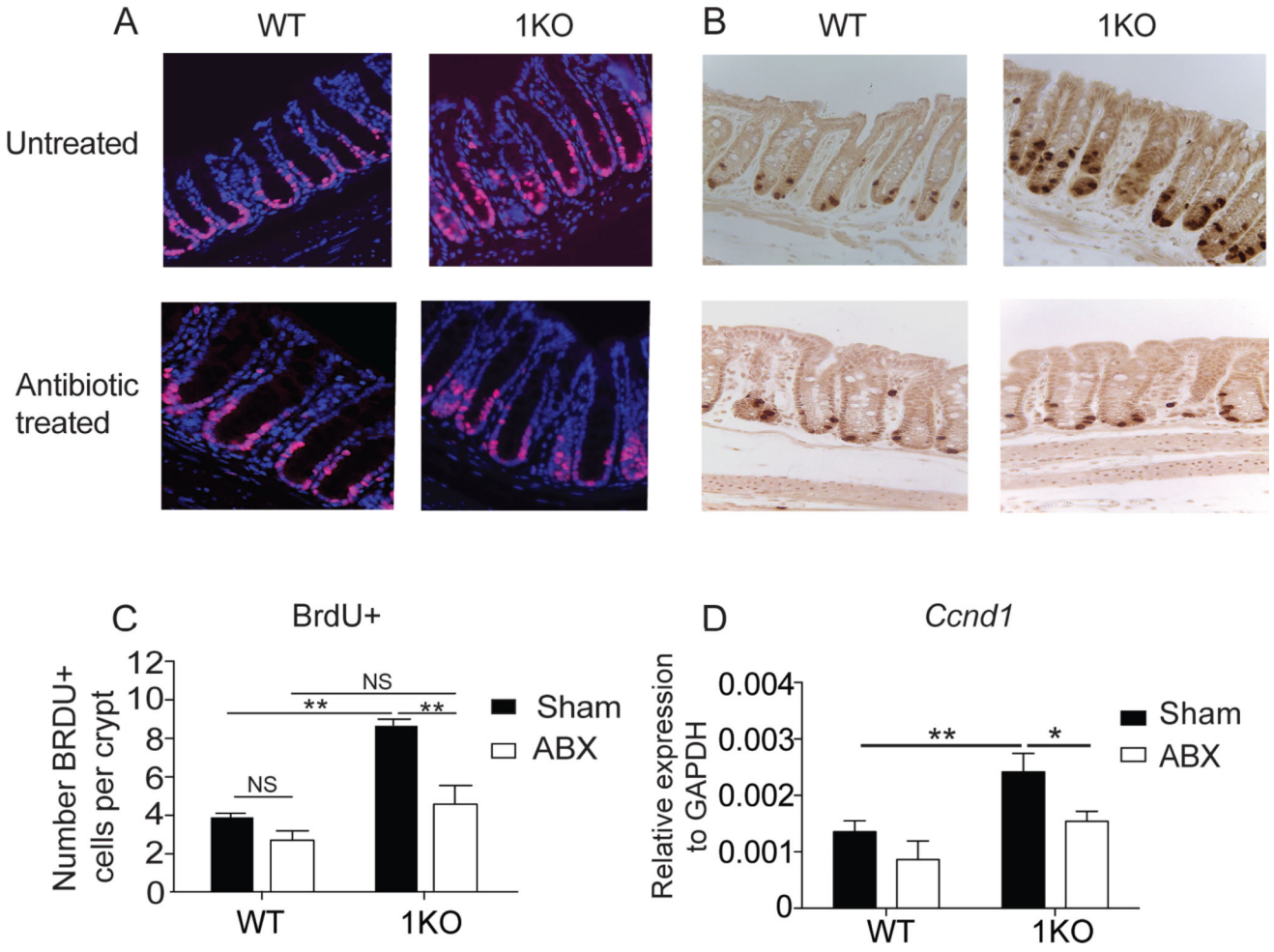

Figure 6. Endogenous TLR1 signaling regulates colonic crypt proliferation

A–C, Histological sections of the colon from 1KO and WT mice under normal SPF conditions or 1KO and WT mice born from a dam receiving antibiotic treated (ABX) water and then maintained on ABX for another two weeks post-weaning. (A) 40X magnification of colon stained with Ki-67. (B) 40X images of colons from mice injected with BrDU 2.5 hours prior to euthanasia. (C) Quantification of total BrdU+ cells per crypt (D) Relative transcript expression of *Ccnd1* in colonic crypts isolated from control and ABX-treated WT and 1KO mice. A, B, representative 40X images taken from 5 mice. C, data is expressed as the mean ± s.e.m. of counts performed independently by 2 two individuals, each counted 30 crypts from 5 mice. D, data is expressed as mean ± s.e.m. from three independent experiments. D, n =5–6 mice per group.; *, $p<0.05$, **, $p<0.01$, ***, $p<0.001$. C, Student's unpaired t-test; D, Two-way ANOVA.

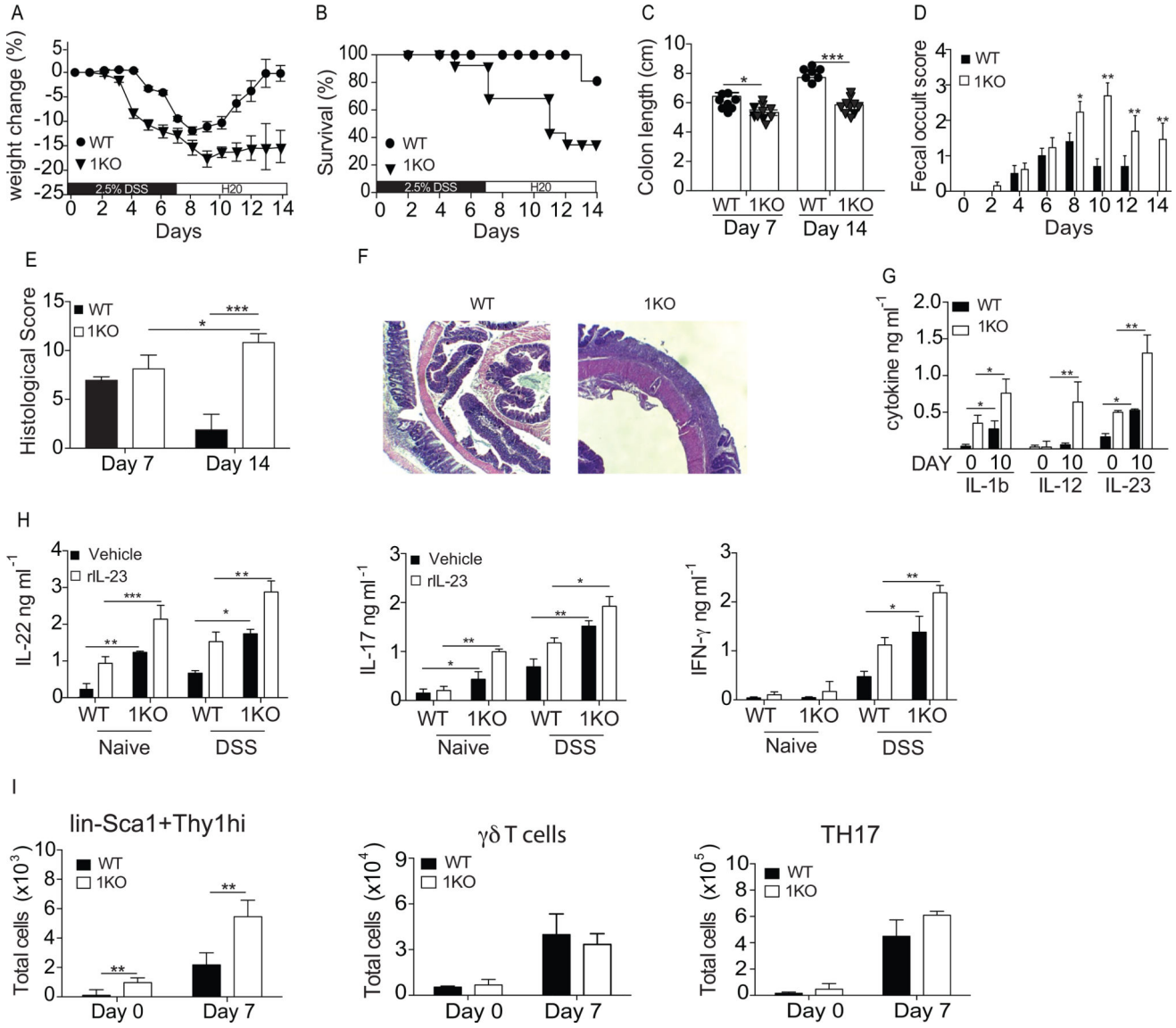

Figure 7. Loss of TLR1 exacerbates DSS-induced cytokine production and prevents colonic repair

WT and 1KO littermates were administered drinking water containing 2.5% DSS for 7 days to induce epithelial injury followed by a 7-day recovery period in which they were returned to normal drinking water. (A) Percent change in weight, (B) survival, (C) colon length at days 7 and 14 (D), fecal occult score. At days 7 and 14 colons were fixed and stained for (E) H&E and (F) histological score was given after analysis by a gastroenterologist. (G) Concentration of IL-1ß and IL-23 found in whole colon homogenates. (H) IL-17, IL-22 and IFN-γ levels from the supernatants of colonic explant cultures derived from naive mice or mice treated with DSS for 10 days. (I) Mean number of cells in the colonic LP determined by flow cytometry for indicated cell type gated as described in Fig 1. legend. A–D, data is expressed as mean ± s.e.m from 3 independent experiments, n=8–10 mice per group. E, the mean of histological scores from 2 independent experiments, n=3 mice per group. F, representative microscopy images of 3 mice per group. G–I, data is expressed as mean ±

s.e.m from two independent experiments with n=6–8 mice per group. A, Wilcoxon log rank test; B, Kaplan Meyer; C, E, G, H, I Students t-test; D, Two-way ANOVA. *, $p<0.05$, **, $p<0.01$. ***, $p<0.001$.

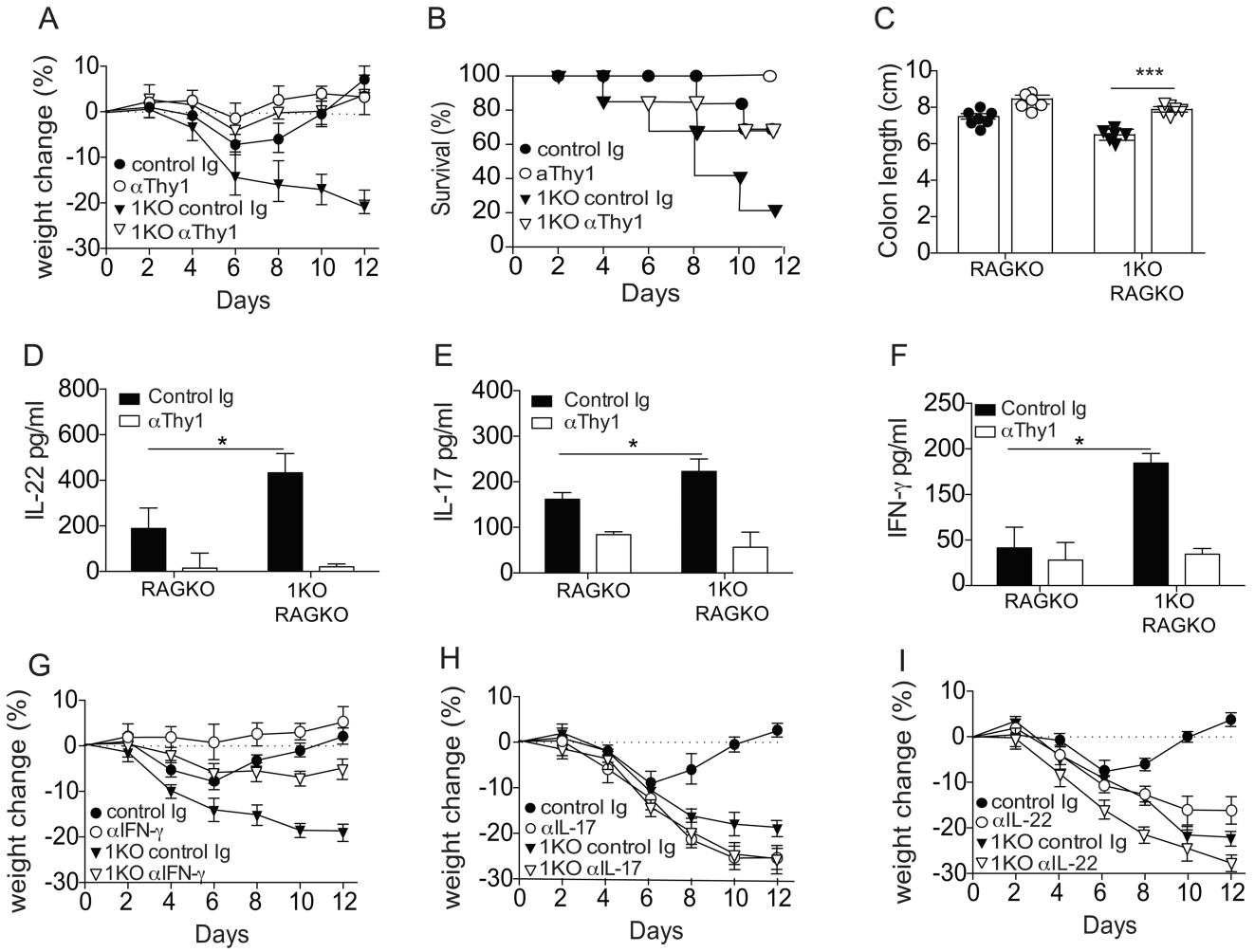

Figure 8. IFN- γ contributes to the mortality observed in the context of TLR1-deficiency

RAG2KO (RAGKO) and TLR1KOxRAG2KO (1KO-RAGKO) were treated with anti-Thy1 depleting antibody every other day beginning on the day of DSS administration through day 12. (A) Percent change in weight, (B) percent survival, (C) colon length at day 12 were assessed. Colonic tissue explants were incubated overnight and the concentration of (D) IL-22 was measured in the supernatant. Levels of (E) IL-17 and (F) IFN-γ levels were determined whole mucosal scrapings. All data is expressed as the mean ± s.e.m. pooled from 2–3 independent experiments. RAGKO and 1KO-RAGKO were treated with polyclonal antibodies against (G) IFN-γ, (H) IL-17 or (I) IL-22 throughout the course of both DSS and recovery and percent change in weight was observed. A, n=7–12 mice per group; B–F I, n=5–7 mice per group. *, $p<0.05$, **, $p<0.01$. Students t-test.